Learning-based vessel segmentaion in mamographic images

Erkang Cheng[1] Shawn McLaughlin[2] Vasileios Megalooikonomou[2]
Predrag R. Bakic[3] Andrew D.A. Maidment[3] Haibin Ling[1]

[1]Center for Data Analytics & Biomedical Informatics, Computer & Information Science Department, Temple University, Philadelphia, PA, USA
[2]Data Engineering Laboratory (DEnLab), Temple University, Philadelphia, PA, USA
[3]Department of Radiology, University of Pennsylvania, Philadelphia, PA, USA

***Abstract*—In this paper we propose using a learning-based method for vessel segmentation in mammographic images. To capture the large variation in vessel patterns not only across subjects, but also within a subject, we create a feature pool containing local, Gabor and Haar features extracted from mammographic images generating a feature space of very high dimension. We also employ a huge number of training samples, which essentially contains the pixels in the training images. To deal with the very high dimensional feature space and the huge number of training samples, we apply a forest with boosting trees for vessel segmentation. Specifically, we use the standard AdaBoost algorithm for each tree in the forest. The randomness is encoded, when training each AdaBoost tree, using randomly sampled training set (pixels) and randomly selected features from the whole feature pool. The proposed method is tested using a real dataset with 20 anonymous mammographic images. The effectiveness of the proposed features and classifiers is demonstrated in the experiments where we compare different approaches and feature combinations. In the paper, we also present full analysis of different types of features.**

***Keywords*-random forest; AdaBoost; vessel segmentation; mammographic images;**

I. Introduction

Mammographic image analysis plays an important role in computer-aided breast cancer diagnosis. Properties of mammographic image such as vessel structures provide basic measurements for anatomic and pathological studies are present in a variety of biomedical contexts of the breast. Patterns of properties such as branching topology, length, spatial distribution, and tortuosity have been analyzed in the literature [1]; alterations in these patterns have been associated with altered function and/or pathology [2], [3].

Vessel segmentation in mammographic images serves as a key step towards automatic or semi-automatic mammographic image analysis. However, this task is challenging because the anatomic vessel structure is usually very complicated in both topology and appearance. In addition, vessel patterns often vary from patient to patient. Even in the same mammographic image, vessel structure can be different for different parts. These challenges even cause difficulties to annotation experts. Fig. 1 gives two examples of mammographic images (top row) and their annotated vessel groundtruth (bottom row).

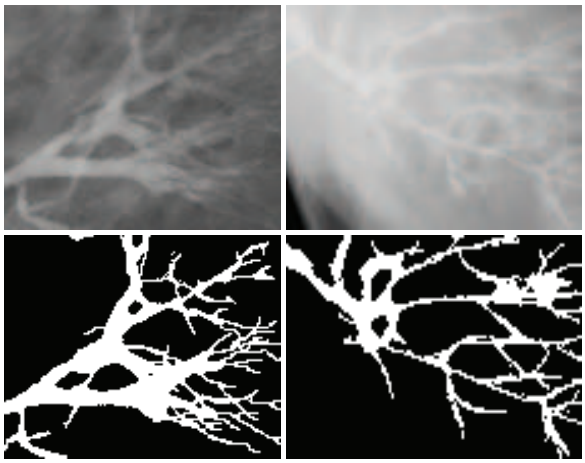

Figure 1. Examples of mammographic images (top row) and annotated vessel groundtruth (bottom row)

Our objective in this paper is to utilize a learning-based approach for the vessel segmentation task in mammographic images. To handle the large variation in vessel patterns, we explore different types of features including local, Gabor and Haar features. As for local features, we use intensities in local regions surrounding a pixel and differential features (e.g. gradients). Haar features are utilized for their ability to capture context information across scales and for their computational efficiency. Gabor features are known for their power in describing across-scale texture patterns. We investigate the performance of these features individually and in combination.

The above mentioned features form a very high dimensional feature space. Furthermore, since we are interested in pixel-wise vessel segmentation, essentially every pixel in the training images serves as a training sample, which consequently leads to a huge set of training samples. Both observations cause practical difficulties to many existing learning-based techniques.

Targeting these challenges, we propose using the random forest framework with a feature pool composed of all local, Gabor and Haar features for vessel detection. We employ the random forest framework because of its known capability to handle both huge number of samples and large feature pools. For each tree in the forest, which we use AdaBoost, not only samples but also features are randomly selected. In the experiments, we compare the proposed method with a single Adaboost tree. We also test the performance of different features. The results clearly demonstrate the effectiveness of our approach.

Furthermore, the random forest and boosting framework provides a natural way to analyze the resulting classifiers, which leads to a comprehensive understandings towards the properties of vessel patterns.

The rest of the paper is organized as follows: In Section 2, we present background information and related work. In Section 3, we introduce the feature pool and the learning framework. Experiments are presented in Section 4. We fully analyze and discuss the effectiveness of proposed features in Section 5. Conclusion is given in Section 6.

II. Background

Vessel structure analysis is an important task in mammographic image analysis, which provides critical information for computer-aided breast cancer detection and diagnosis. As a result, vessel segmentation has been attracting research efforts for many years. Early works usually involve manual or semi-automatic efforts, often combined with vessel specific enhancement.

Leaning-based techniques play an important role in recent vessel anatomy studies (e.g., [6], [7], [9]). Staal et al. presented an algorithm to detect vessel based on using ridges as features [6]. KNN was used to train a classifier which is utilized for classifying the vessels and the background. A hierarchical model with learning-based method was studied in [7]. Haar-like and steerable features were used in their work. Clear boundary points were needed in their method.

Similar work has been done in retinal and blood vessel detection. Some approaches focus on image processing technoques such as using Gaussian kernel to do the preprocessing [4]. Other approaches involved region growing methodologies [5]. The shape model was also introduced to achieve vessel segmentation. Shape prior and contour information was explored in [8] where experiments were performed on both 2D and 3D data.

The proposed method is motivated by these studies. Our main focus is on automatic vessel segmentation using an effective ensemble learning framework. In addition, we also evaluate the effects of several important features.

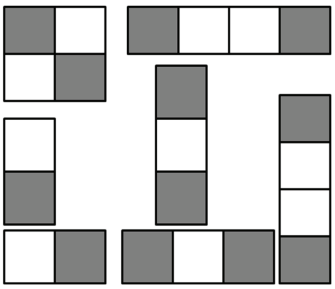

Figure 2. Haar-like filters

III. Methodology

A. Feature Pool

In this section we describe the three different types of features used in our proposed framework. Our final goal is two-fold: to use these features for building robust vessel segmentation algorithms and to analyze the roles of these features in the algorithms.

1) Local features: In Fig. 1, vessels are shown as the brightest areas in mammographic images. This is because vessels are filled by a contrast agent in the capturing step. Intensity and its variation can also be utilized as features [9].

Given an image I, we consider $I(x, y)$, $I_x(x, y)$, $I_y(x, y)$, $I_{xx}(x, y)$, $I_{xy}(x, y)$ and $I_{yy}(x, y)$ as local features, where I is intensity, I_x, I_y denote the image gradients along horizontal and vertical directions, I_{xx}, I_{yy} and I_{xy} denote the second derivatives. In addition, the Laplacian $L(x, y)$ and the eigen values Hessian matrix $H(x, y)$ are included in the local feature pool.

It is apparent that neighbor information is meaningful because those vessel pixels are always connected with their neighbors. In order to capture the context information in the images, a patch-based method is used to extract such local features. When we calculate local features for a pixel in the mammographic image, values of neighbors covered by an $N \times N$ rectangle are also taken into account. In addition, statistical values, i.e., average and standard deviation in the rectangle are included into the local feature space.

2) Haar features: Haar-like features (Haar features for short) have been successfully used in the first real-time face detector [10]. Taking benefit of the integral images, a Haar feature can be calculated efficiently in constant time. The computation of Haar features is through the Haar-like filters as shown in Fig. 2.

Fig. 2 illustrates seven types of Haar-like filters. In this figure, the sum of the pixels lying inside the white rectangles is subtracted from the sum of the pixels lying within the grey rectangles. More spaciality, the value of a two-rectangle feature is the difference between the sum of the pixels within two rectangular regions. The regions have the same size and shape and are horizontally or vertically adjacent. A

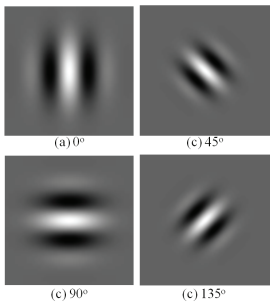

Figure 3. Gabor filters along different orientations

three-rectangle feature computes the sum within two outside rectangles subtracted from the sum in a center rectangle. Finally a four-rectangle feature computes the difference between diagonal pairs of rectangles or two outside rectangles. Given a patch size is 15×15, the number of combinations of rectangles is exhaustively large.

The width of vessel structures varies a lot depending both on patients and on locations within a mammographic image. To handle this variation, we collect Haar features at different scales within a patch centered at each pixel. Haar features provide a bunch of combination of rectangles shown in Fig. 2. Some combinations weakly simulate different vessel structures in mammographic images.

3) Gabor features: Gabor wavelet is known to be very effective for texture representation [13]. Compared with Haar features, Gabor features capture additional information from the frequency domain.

The real and imaginary Gabor filters are expressed as:

$$Gabor^r(u,v,\lambda,\theta,\varphi) = \exp(-\frac{u'^2}{2\delta_x^2} - \frac{v'^2}{2\delta_y^2})\cos(2\pi\frac{u'}{\lambda} + \varphi)$$

$$Gabor^i(u,v,\lambda,\theta,\varphi) = \exp(-\frac{u'^2}{2\delta_x^2} - \frac{v'^2}{2\delta_y^2})\sin(2\pi\frac{u'}{\lambda} + \varphi)$$

where $u' = u\cos\theta + v\sin\theta$,$v' = -u\sin\theta + v\cos\theta$ (u,v) is the relative coordinate using (x,y) as origin, and λ, δ and φ are the spatial frequency, standard deviation (along x and y axes), and shift, respectively.

Examples of Gabor filters are showed in Fig. 3. It shows four Gabor filters of wavelength of 5, δ_x,$\delta_y = 1/2$, and rotations at 0, 45, 90 and 135 degrees respectively.

Gabor features are popular used in vessel segmentation or extraction [13], [14], [15] due to their directional selectiveness capability. Gabor filters provide responses along different orientations. Vessels have strong orientation information in mammographic images. Consequent results of Gabor filters produce rich information about vessel orientation.

To compute Gabor features, an input image is convoluted with real and imaginary Gabor filters along a direction θ. For each pixel, amplitudes of these outputs is calculated as Gabor feature related to direction θ. Besides responses at a pixel, the responses of its neighbors covered by an $N \times N$ patch are also taken into consideration to enhance the descriptive power. In particular, this kind of information enables our method to encode context information for segmentation.

B. Learning framework

For each pixel in a mammographic image, the features presented in the above subsection forms a huge feature pool. Furthermore, we also have a huge number of samples that are essentially all the pixels from the training images. We choose the random forest framework for this learning task due to its flexibility and its excellent performance in many recent applications.

The random forest framework is an ensemble classifier consisting of N decision trees which outputs the class that is the mode of the class's output by individual trees [11]. Associated with each tree i is a learned class distribution $p(c|i)$. In each tree, a subset of training samples is randomly drawn from the whole training set. For each node in the forest, a subset of features is randomly chosen as input. The best feature from the randomly selected features is calculated based on the gini index. Then a tree is grown based on the new training set using random feature selection. The trees grown are not pruned.

The benefit of random forest lies in that it can handle a large training set using a large feature set. Another advantage of the random forest framework is that trees in the forest can be processed in parallel. In the training stage, we can train each tree parallel. The predicting step can be conducted simultaneously. Random forests has been successfully applied to medical image analysis in various tasks [16], [17].

We adapt the random forest framework to a forest with boosting trees in it. In our implementation, we use Adaboost classifiers instead of decision trees as members of the random forest. Adaboost is an efficient ensemble learning method that builds a strong classifier as a linear combination of a set of weak classifiers [12]. Specifically, let $x \in \Re^d$ be a d dimensional input feature vector, the final (strong) classifier $h(x) : \Re^d \rightarrow \{-1, 1\}$ has the following form:

$$h(x) = \sum_{i=1}^{n} c_i h_i(x)$$

where $h_1(x), \cdots, h_n(x)$ are the n weak classifiers.

Fig. 4 gives an illustration of the random forest framework. Training process is shown with solid blue line. Dash line represent inference pipeline when a testing instance comes.

In the training step, for each tree in the forest, samples are randomly selected from the whole training set. Features used in each tree are also randomly sampled from the feature pool. This strategy has the ability to solve the problem of having both a huge number of samples and a huge number

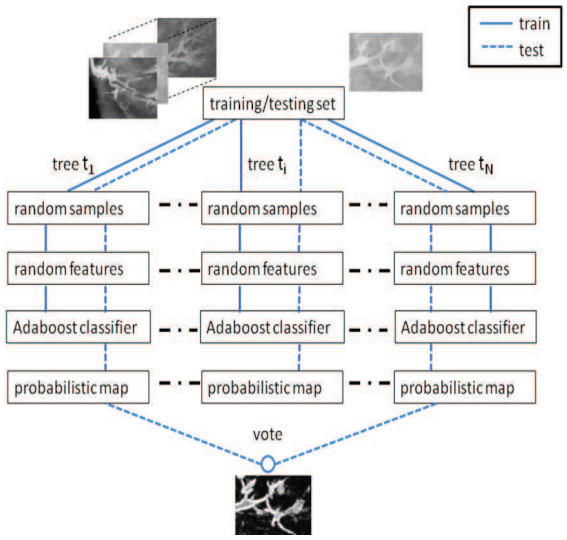

Figure 4. The learning and inference framework

of features for each instance. Each tree is recognized as an Adaboost classifier. Certain numbers of weak classifiers are selected in each tree to be combined into a strong classifier. The features responding to these weak classifiers help us analyze the importance and effectiveness of each feature in the whole feature space.

After training all Adaboost classifiers in each tree, the inference is performed based on voting by these classifiers. Given a testing instance, in the testing process, features are sub-sampled from the entire feature space. These sub-sampled features are the same as the ones used in the training approach. For each pixel x in a given new image, we use probabilistic responses (through logistic transformation) for each Adaboost tree.

$$p_i(vessel|\mathbf{x}) = \frac{e^{h_i(\mathbf{x})}}{1 + e^{h_i(\mathbf{x})}}$$

Each boosting tree provides a probability value of the pixel being inside a vessel. The final random forest result is the average of probabilistic maps over all the Adaboost outputs

$$p_{final}(vessel|\mathbf{x}) = \frac{1}{N}\sum_{i}^{N} p_i(vessel|\mathbf{x})$$

where N is the number of trees in the random forest, and $p_i(x)$ is the probabilistic map of the i-th Adaboost classifier. Pixels with higher probability value indicate a higher chance to be inside vessels in mammographic image. As in the random forest framework, the training and testing process can be parallelized in the whole experiments.

C. Evaluation

The final vessel segmentation can be obtained by selecting thresholds based on the average probabilistic map.

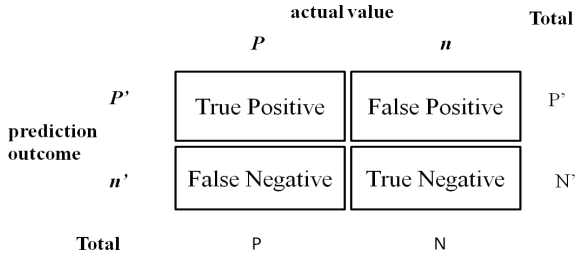

Figure 5. Components for calculating ROC curve

For the evaluation task, the equal error rate (EER), is defined as the error rate when a threshold generates the same correct acceptance rate (CAR) and correct rejection rate (CRR), which are defined as:

$$CAR = \frac{correctly\ \ acceptly\ \ vessel\ \ pixels}{all\ \ vessel\ \ pixels}$$

$$CAR = \frac{correctly\ \ rejected\ \ non-vessel\ \ pixels}{all\ \ non-vessel\ \ pixels}$$

The ROC curve is also provided as an evaluation criterion. It is based on true positive rate and false positive rate calculated as follows:

$$True\ \ positive\ \ rate = \frac{True\ \ Positive}{Total\ \ Number\ \ of\ \ Positive}$$

$$False\ \ positive\ \ rate = \frac{False\ \ Positive}{Total\ \ Number\ \ of\ \ negative}$$

where, true positive and false positive are explained in Fig. 5. Total number of positive is the number of vessel pixels in the whole dataset. Number of non-vessel pixels in the all mammographic images is represented as total number of negative.

When vessel probabilistic maps are predicted with learned classifiers, we can get binary images using different thresholds. In the probabilistic map, all the values are between 0 and 1. We use thresholds between 0.01 to 0.99 and set the interval to 0.01. The result for each threshold provides values in Fig .5 to calculate the ROC curve.

Using these different thresholds, we could can generate an ROC curve. The horizontal axis is the false positive rate and the vertical axis is the true positive rate.

IV. Experiment Results

A. Experiment Setup

The dataset we used in the experiments consists of 20 anonymous mammographic images.

To calculate local features for each pixel, a patch of size 15×15 centered at each pixel is used. Responses of all the pixels together with the mean and standard derivation for each patch are used. This generates 1818 local features.

The dimension of Haar features for one pixel is 7056 using patch size of 15×15. There are seven different types

Table I
NUMBER OF FEATURES USED IN EACH APPROACH

Training set	Random Boosting Forest	Adaboost
Local	145	1818
Haar	564	7056
Gabor	290	3632
All	1000	12506

of Haar features as shown in Fig. 2. A Haar feature generates a lot of Haar-like shapes at different location and different sizes. The combination of these features simulate the vessel structures to a certain degree. Through feature selection, most discriminative features at certain position and certain size are chosen in the training step.

The Gabor filters are of size 15×15 and the parameters used are combinations of $\delta_x, \delta_y = 1/2, 1/16$, and four angles (0, 45, 90 and 135 degrees). For each pixel, we also collect neighbors covered by a 15×15 rectangle centered at this pixel. Similarly to calculate local feature, the mean and standard derivation within the rectangle are chosen as features. That gives 3632 Gabor features in total for each pixel in the mammographic image.

Combining local, Haar and Gabor features together, we have a large feature pool of size 12506. Our learning framework is able to select most important features from the original large feature pool.

To study the effectiveness of the proposed learning and inference framework, we compared random boosting forest with a single Adaboost. For random boosting forest, we used 64 Adaboost classifiers, each of them having 50 weak classifiers. Each weak classifier is responded to one kind of feature in the feature space. That means we have 64 boosting trees in the forest and each tree trains an Adaboost classifier with 50 weak classifiers in it.

For each tree in the boosting forest, 10000 samples are randomly selected for training each Adaboost classifier. For both random forest and single Adaboost, we also tested effectiveness of different features. In summary, there are two different classifiers and four different feature sets tested in our experiments, resulting in eight different configurations. These configurations and corresponding number of features are summarized on Table I.

For each tree in the boosting forest, features are randomly selected as input. Column 2 in Table I shows the number of randomly selected features used in the random boosting forest. The number of features in total for each combination are listed in the column 3 of Table I. These features are used in single Adaboost.

B. Experimental Results

We used 4-fold cross validation for evaluating different configurations. In each fold, 15 mammography images were used for training and the remaining 5 images were used for testing. For each training/testing combination in each folder,

Table II
EQUAL ERROR RATES OF DIFFERENT METHODS

Feature	Random Boosting Forest	Adaboost
Local	10.94%	14.58%
Haar	10.66%	14.03%
Gabor	10.41%	12.32%
All	**10.06%**	**12.19%**

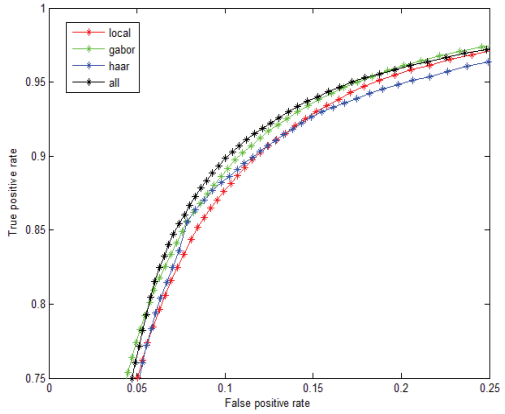

Figure 6. ROC curve of four different feature configurations using random forest framework

we test all different configurations described above. The equal error rates for different combinations are presented in Table II.

In the random forest method, we calculate the ROC curve for each of these four different configurations. Fig .6 displays the ROC curves in different colors.

Table II and Fig. 6 shows that when we use the random forest as the learning and inference framework, the best result is archived by using all the features as input. In other words, combination of local, Haar and Gabor features generates better results than using each type of features individually. Another observation is that Gabor features perform better than do the local and Haar features. This is because that Gabor features have orientation selection capability. The observation implies that Gabor features capture the tree-like pattern which is the most important property of vessels in mammographic images. Besides considering local texture based on intensity, the Haar-like feature also includes width information of vessels under various scales.

We also compare the effectiveness of random forest with boosting trees and using single Adaboost as classifier. We compare their results both using all features as input. Simply, the single AdaBoost is a tree in the random forest.

Fig. 7 shows results (probabilistic maps) on testing images with random forest and single AdaBoost as classifier. The first row is the original image. The second row gives the result using random forest with 64 boosting trees in it. Probabilistic maps tested with single AdaBoost is provided

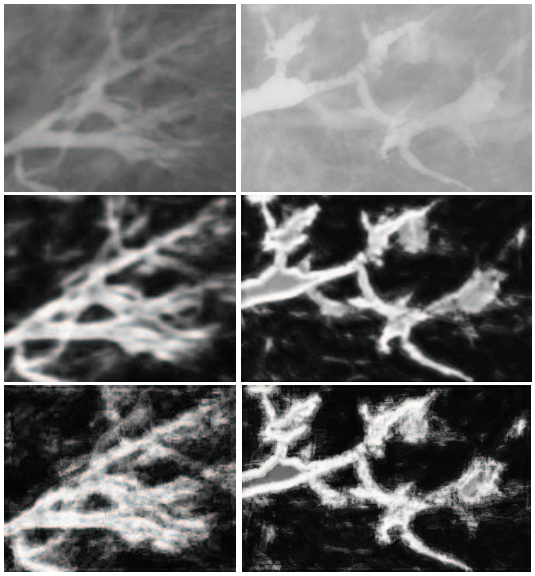

Figure 7. Input images (first row) and the probabilistic maps of random forest (middle) and Adaboost (bottom). Both results use all features. Higher intensity of probabilistic map indicates high possibility of a vessel being present.

in the last row.

Examples in Fig. 7 clearly demonstrate the effectiveness of the proposed method. We have the following observations: for all feature combinations, the random forest consistently outperforms a single Adaboost. This agrees with our motivation for using random forest since it effectively handles a large number of features and samples.

V. Analysis and Discussion

A. Results of different features

In this section, we analyze the weak classifiers chosen in the random boosting forest. Each classifier is corresponding to one type of features in the entire feature space. We have 64 boosting trees in the forest and each tree train a AdaBoost classifier. In the training stage, each tree selects 50 features from randomly sub-sampled feature space as weak classifiers. Each selected feature is considered as a weak classifier. These 50 selected weak classifiers are combined to form a strong AdaBoost Classifier. Together with four-fold cross validation, $64 \times 50 \times 4 = 12800$ features are selected as weak classifiers in the experiment. These chosen features help us to evaluate different types of features.

Fig. 8 illustrates the percentages of different kinds of features being selected as weak classifiers and the ratios in the whole feature space individually. In the three different types of features, Gabor features are the features chosen the most in all the weak classifiers. The ratio of Gabor features in the feature pool is less than the ratio that they are being selected as classifiers. Ratios of Haar and local feature in the whole feature space are higher than the percentages being

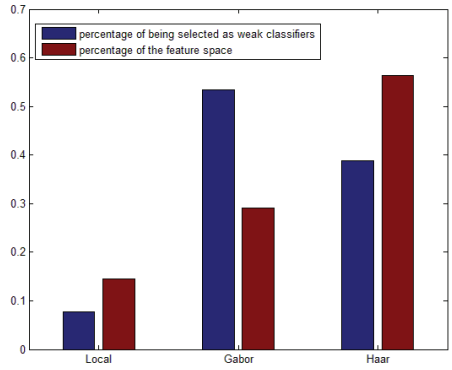

Figure 8. Percentages of different kinds of features being selected as weak classifiers (blue) and the ratio in the whole feature space (brown).

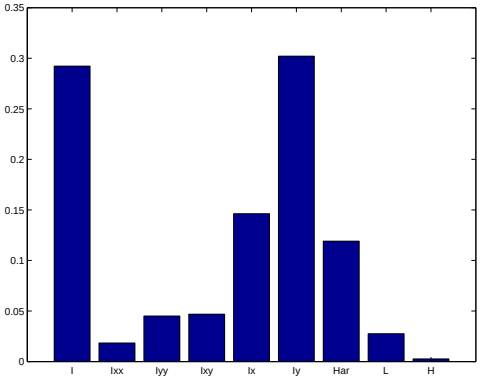

Figure 9. Histogram of each local feature being selected as weak classifier

selected as weak classifiers. This explains Gabor feature performs better than other features in the experiments.

In the following parts, we also analyze three different features individually with random boosting forest as learning and inference framework.

B. Importance of local features

As description in Section III-A1, there are 9 types of features in all the local feature space. With random forest with 64 trees in it, 12800 features are chosen in the training step. We group these selected features into 9 categories. Histogram of ratio of each component in the local feature is presented in Fig .9.

In local feature pool, the three most chosen features are gradient I_y, Intensity I and gradient I_x. Intensity is apparent as characteristic in mammographic images This is true because vessels with bright intensity in mammographic images which are obtained by agent projected via x-rays. Gradient I_x and I_y information demonstrate that vessels vary along certain directions. There are significant of vessels in mammographic images.

Fig. 10 comprehensively illustrates the importance of all

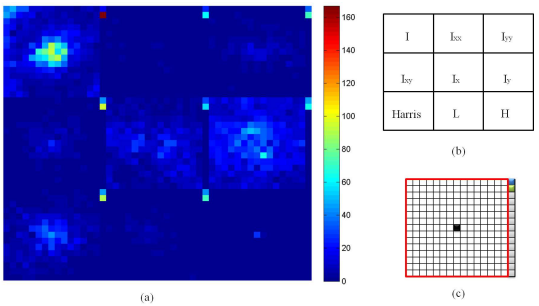

Figure 10. Weight of each feature being selected in the local feature space

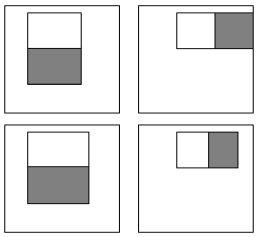

Figure 11. The four most frequently selected Haar features

the features in the local feature space. In Fig. 10 (a), each local feature is given a weight of being selected in the training approach. Bright color indicates features that are more discriminative than features with darker color. Fig. 10 (b) explains the structure of Fig. 10 (a). Each block in Fig. 10 (a) represents one group feature in local feature pool. Fig. 10 (c) shows the context in each block of Fig. 10 (a). Each block is of size 15×16. The first 15×15 elements denote the importance of itself and its neighbors. Pixels covered by the red rectangle is the neighbors of the centered (black) pixel. The first two values in the 16 column is the importance of mean (blue) and standard deviation (green) within the neighborhoods.

For local feature, we collect values in 15×15 neighborhoods. Weight of each block infers that the statistical values are always more significant than the individual value in the block. Fig. 10 (a) shows that the most discriminative neighbor size is around 5×5.

C. Importance of Haar features

With a patch size of 15×15, we collect 7056 features totally using seven different types of Haar-like features. Configurations of Haar features simulate the tree-like vessel structure in mammographic images. In combination with Adaboost used as a classifier in each tree, most important features are selected as weak classifiers. Using Haar features and random boosting forest as framework, 50 Haar-like features specified by its location and shape in the 15×15 patch are chosen to form the strong classifier in each tree. We count the frequencies of each Haar-like feature and show the four most chosen features in Fig. 11.

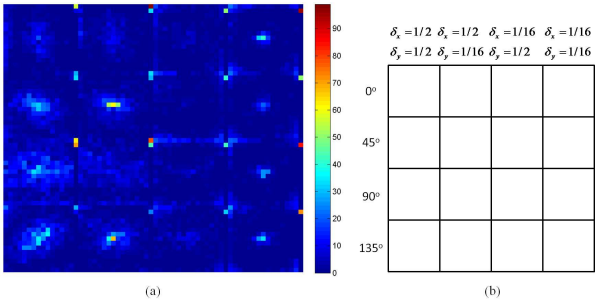

Figure 12. Feature importance in Gabor feature space.

Fig. 11 shows the top four Haar features chosen in all the weak classifiers. First row is the top1 and top 2 selected features. Top3 and top 4 chosen features are shown in the second row.

In the experiment, the patch to calculate Haar features of size 15×15. The location of these top 1 and top 3 features in the 15×15 patch is $(1, 3)$ along vertical and horizontal directions. The top 2 and top 4 chosen features are in location $(1, 5)$. The sizes of shape which represent the top 4 Haar features are 10×7, 5×10, 10×8 and 4×10.

The shapes of these top 4 selected features indicate that the most likely width of vessel is around 5×5. This is similar as we prove in the local feature; the most discriminative neighbor size is around 5×5. These four shapes of chosen most features indicate that Haar features simulate vessels go along horizontal and vertical directions. This confirms in local feature pool, gradient I_y and I_x are much more significant than other groups of features.

D. Analysis on Gabor features

The 2D Gabor filters are of size 15×15 and the parameters used are combinations of $\delta_x, \delta_y = 1/2, 1/16$, and four angles $(0, 45, 90\ and\ 135$ degrees). We group Gabor features into 16 categories. Like local features, weight of each Gabor feature is shown in Fig .12 (a).

There are 4×4 blocks in Fig .12 (a). The structure is explained in Fig. 12 (b). Rows of blocks are features along 0, 45, 90 and 135 degrees, respectively. The combinations of different variation of horizontal and vertical orientation of Gabor filters are shown in the upper part of Fig. 12 (b).

For extracting Gabor features, values in neighborhood of $15 \times$ 15 are collected. In addition, statistical values of the patch are taken to extend the power of features. Context of each block is the same as shown in Fig. 10 (c). Like analyzed in local features, most statistical values are always discriminative.

Weights being selected in the training stage of categories in Gabor features are compared and evaluated. The histogram of these weights is provided in Fig. 13. We extend the groups of features shown in Fig. 12 by row to get the weight of their importance.

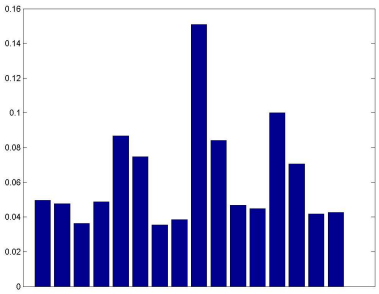

Figure 13. Histogram of each Gabor feature being selected as weak classifier.

By comparing the types of features grouped by orientation and derivation in horizontal and vertical directions, we see that the most chosen gabor feature is along 90, 135 and 45 degrees with $k_x = 1/2$ and $k_y = 1/2$. The fact that 90 degrees is chosen proves that gradient I_y is the most important feature in local feature space. Orientations 45 and 135 mean that the vessels always go along these directions.

Also, from the block of Fig .12 (a), we can conclude that the most interesting neighborhoods size is around 5×5. This holds among local, Haar and Gabor features.

E. Summary on analysis of features

In collusion, our analysis shows orientation and context information plays an important role in vessel segmentation. In addition, the most discriminative neighborhood size is 5×5.

VI. Conclusion

In this paper we propose using a learning-based method for vessel segmentation in mammography images. More specifically, we employ the random boosting forest framework that uses Adaboost classifiers as members. In addition, we use a combination of three types of features for vessel description. The proposed method was evaluated in a real dataset with different feature combinations. Its effectiveness was observed in the experiments and was compared to that of a single Adaboost classifier. Moreover, we evaluate different features in the paper. In the future, we plan to explore high-level context models.

VII. Acknowledge

We thanks anonymous institute for providing mammographic images and anonymous experts for the annotations. This work was supported in part by NSF Research Grant IIS-0916624. The funding agency specifically disclaims responsibility for any analysis, interpretations and conclusions.

References

[1] Uppaluri, R., Hoffman, E.A., Sonka, M., Hunninghake, G.W, McLennan, G., Interstitial Lung Disease: A Quantitative Study Using the Adaptive Multiple Feature Method, Am. J. Respiratory.

[2] K Horsfield and A Thurlbeck, "Relation between diameter and flow in branches of the bronchial tree," Bulletin of Mathematical Biology, 43 (6), 681-691, 1981.

[3] V. Megalooikonomou, M. Barnathan, D. Kontos, P. R. Bakic, A. D.A. Maidment, "A Representation and Classification Scheme for Tree-like Structures in Medical Images: Analyzing the Branching Pattern of Ductal Trees in X-ray Galactograms," IEEE Trans. on Medical Imaging, 28(4):487-493, 2009.

[4] R. Zwiggelaar, T. C. Parr, and C. J. Taylor, "Comparing line detection methods for medical images," Int'l Conf. of the IEEE Eng. in Med. and Bio. Soc., vol. 3, 1161-1162, 1996.

[5] X. Y. Jiang and D. Mojon, "Adaptive local thresholding by verification-based multithreshold probing with application to vessel detection in retinal images," IEEE Trans. on Pattern Analysis and Machine Intel., vol. 25, 131-137, 2003.

[6] J. Staal, M. D. Abramoff, M. Niemeijer, M. A. Viergever, and B. van Ginneken, "Ridge-based vessel segmentation in color images of the retina," IEEE Trans. on Medical Imaging, vol. 23, pp. 501-509, 2004.

[7] R. Socher, A. Barbu, D. Comaniciu, "A learning based hierarchical model for vessel segmentation". IEEE Int'l Symposium Biomedical Imaging, 1055-1058, 2008.

[8] Nain, D., Yezzi, A., and Turk, G. "Vessel segmentation using a shape driven flow," Intl. Conf. on Medical Image Computing and Comp. Ass. Intervention, 51-59. 2003.

[9] H. Ling, M. Barnathan, V. Megalooikonomou, P. Bakic, A.Maidment. Probabilistic branching node detection using local hybrid features. IEEE Int'l Symposium on Biomedical Imaging, 2009.

[10] P. Viola and M. Jones, "Rapid object detection using a boosted cascade of simple features," CVPR, 2001.

[11] Breiman, L.: "Random forests." Machine Learning 45(1), 5-32, 2001.

[12] Y. Freund, R. E. Schapire: A Decision-Theoretic Generalization of On-Line Learning and an Application to Boosting. J. Comput. Syst. Sci. 55(1): 119-139. 1997.

[13] Soares, J.V.B.; Leandro, J.J.G.; Cesar, R.M.; Jelinek, H.F.; Cree, M.J.; , "Retinal vessel segmentation using the 2-D Gabor wavelet and supervised classification," IEEE Transactions on Medical Imaging, 25(9:1214-1222, 2006.

[14] Cemil Kirbas and Francis Quek. "A review of vessel extraction techniques and algorithms". ACM Computing. Surveys. 36, 2, 81-121, 2004.

[15] B. Zhang, L. Zhang, L. Zhang and F. Karray, "Retinal Vessel Extraction by Matched Filter with First-Order Derivative of Gaussian," Computers in Biology and Medicine, 40(4):438-445, 2010.

[16] A. Barbu, M. Suehling, X. Xu, D. Liu, S. K. Zhou, D. Comaniciu. Automatic Detection and Segmentation of Axillary Lymph Nodes. In MICCAI, 28-36, 2010.

[17] Criminisi, A., Shotton, J., Robertson, D., Konukoglu, E.: Regression Forests for Efficient Anatomy Detection and Localization in CT Studies. In: MICCAI Workshop on Recognition Techniques and Applications in Medical Imaging, 2010.